Recognition of children's movement patterns during recess for characterizing particle exposure doses

Build Simul
https://doi.org/10.1007/s12273-025-1295-x

Recognition of children's movement patterns during recess for characterizing particle exposure doses

Feng Yuan[1,2], Runming Yao[1,2,3] (✉), Prashant Kumar[4,5], Christopher Pain[6], Ziyu Shu[1,2], Baizhan Li[1,2]

1. *Joint International Research Laboratory of Green Buildings and Built Environments (Ministry of Education), Chongqing University, Chongqing 400045, China*
2. *National Centre for International Research of Low-carbon & Green Buildings (Ministry of Science and Technology), Chongqing University, Chongqing 400045, China*
3. *School of the Built Environment, University of Reading, UK*
4. *Global Centre for Clean Air Research (GCARE), School of Sustainability, Civil and Environmental Engineering, Faculty of Engineering and Physical Sciences, University of Surrey, Guildford GU2 7XH, UK*
5. *Institute for Sustainability, University of Surrey, Guildford GU2 7XH, UK*
6. *Department of Earth Science and Engineering, Imperial College London, London SW7 2AZ, UK*

Abstract

Children exhibit unique activity patterns in classrooms, and their movements influence the resuspension of particulate matter, thereby increasing the risk of inhalation. To quantify children's activity patterns and particulate matter inhalation doses, we measured particulate matter concentrations and tracked the recess activities of 194 children in two primary schools. YOLO v9 combined with the DeepSORT algorithm was used to identify and track the children in the videos, thereby calculating the speed and duration of each child. Statistical analysis revealed that classroom activities were highly transitory and predominantly of light intensity. The proportion of light-intensity physical activity in this study was 7%–15% higher than that reported in previous studies, attributable to high occupant density, limited activity space, and characteristics of the Chinese education environment. The median durations of recess activities decreased from light-intensity (4.7 s) to moderate-intensity (2.5 s) and vigorous-intensity activities (2.2 s). Furthermore, children's activity speed and duration were strongly associated with variations in indoor PM2.5 concentrations. Additionally, the daily inhalation dose during recess decreased with increasing age, being 14.67% lower in the middle age group and 30.64% lower in the upper age group compared to the lower age group. Our analysis provides a valuable reference for assessing the health risks caused by particulate matter and for more effective measures to improve the classroom environment.

Keywords

activity speed
activity duration
machine learning
primary school
particulate matter exposure

Article History

Received: 21 January 2025
Revised: 25 March 2025
Accepted: 23 April 2025

1 Introduction

Particulate matter (PM) pollution has been identified as a significant source of indoor air pollution in primary school environments (Xu et al. 2018; Kumar et al. 2024). Children spend up to 10 hours per day in school environments, primarily indoors (Oliveira et al. 2019). Consequently, classrooms are recognized as a critical built environment due to the potential for adverse indoor conditions to impact children's health, comfort, and academic performance (Sadrizadeh et al. 2022). Moreover, classrooms typically have higher occupant densities than family residences, and it is precisely the presence of occupants and their activities that are key factors influencing PM levels (Diapouli et al. 2007; Zhong and Ridley 2020; Yuan et al. 2024). Recess breaks, which are the only periods of relatively unstructured time in the school day, significantly influence physical activity levels in schools, characterized by frequent, intense bursts

E-mail: r.yao@cqu.edu.cn

of activity, particularly when children play indoors (Ruch et al. 2013; De Baere et al. 2015). Children exhibit higher activity intensity than teenagers and young adults (Sigmund et al. 2007; Livingstone et al. 2003). These factors contribute to elevated PM concentrations in classrooms during recess (Madureira et al. 2012; Yang et al. 2023).

Existing research has demonstrated that activity speed is a crucial factor influencing PM concentration, with higher speeds enhancing PM resuspension (Boulbair et al. 2022; Um et al. 2022; Yuan et al. 2024). However, most studies do not consider the characteristics of children's activities during recess and the variability between different age groups. Research on children's activity patterns indicates that their daily activities are characterised by brief periods of high-intensity activity, interspersed with short, irregular bouts of moderate to light-intensity activity, overall showing a large proportion of light-intensity activity, high intermittency, and brevity (Rowlands and Eston 2007; Chinapaw et al. 2019; Xie et al. 2024). Yet, most of the existing research has focused on statistics of children's daily activities without differentiating between indoor and outdoor classroom activities. Additionally, significant differences in children's activity patterns exist between different school types, such as kindergarten and primary school (Branco et al. 2019; Zhou et al. 2021). Therefore, there is a need to quantify children's movement patterns during recess activities in primary school classrooms.

The growing interest among researchers in dynamically monitoring children's activities has led to the widespread use of devices such as pedometers and accelerometers (Rowlands and Eston 2007; Gu et al. 2024). However, the cost of these monitoring devices remains a significant barrier, particularly for studies involving large cohorts of children. In addition to expensive devices, video analysis has emerged as a primary method for human activity analysis in computer vision (Turaga et al. 2008; Cristani et al. 2013). Among various video-based approaches, the YOLO series is a leading choice for real-time object detection, widely used for its efficiency and accuracy (Redmon et al. 2016; Wang et al. 2023; Wang et al. 2024b). The integration of YOLO with the DeepSORT framework enables real-time detection of trajectories and tracking of individuals based on speed, distance, and physical appearance (Azhar et al. 2020; Punn et al. 2021; Ghomashchi et al. 2024).

Activity patterns in specific environments significantly influence PM exposure doses (Du et al. 2024). Children's exposure to pollutants is determined by the activity type, location, and intensity (Cohen et al. 2000; Kim et al. 2019; Li et al. 2023). The duration and frequency of time spent in specific locations result in different exposures and risks to children that vary with age and development stage (Cohen et al. 2000). However, no studies have yet investigated how children's activity patterns during classroom recess influence PM exposure discrepancies. Therefore, it is essential to characterize children's movement patterns and quantify exposure doses during recess in high-occupancy, limited-space classrooms.

In this study, PM2.5 monitors were used to assess real-time PM2.5 concentration in primary schools. Children's recess activities were recorded via cameras and analysed using machine learning algorithms, allowing us to examine the contribution of different activity patterns to PM2.5 exposure across various age groups. The main objectives of this study are: (1) to develop a framework for extracting activity speeds and durations using machine learning algorithms for human recognition, tracking, and coordinate transformation; (2) to quantify the speed, intensity, and duration of recess activities among children of different age groups; and (3) to investigate PM2.5 inhalation doses and their variability in children of different age groups based on the acquired activity patterns and measured PM2.5 concentrations.

2 Methodology

2.1 PM2.5 concentration measurement and activity video collection

2.1.1 Characteristics of studied classrooms

The field study was conducted from September to December 2023. Two public primary schools in China, one in a rural area of Chongqing and the other in an urban area of Ziyang City, Sichuan Province, were selected as experimental sites. Figure A1, which is available in the Electronic Supplementary Material (ESM) of the online version of this paper, illustrates the geographic locations of School A and School B. A total of six classrooms, varying in school location, number of students, occupant density, and grade levels, were included in this study. Specifically, three classrooms for Year 2, Year 3, and Year 6 were chosen in School A, and three classrooms for Year 1, Year 4, and Year 5 were chosen in School B. The average number of students per classroom, classroom area, and occupant density were 32 people, 49.10 m^2, and 1.9 m^2/person, respectively. Both schools rely on natural ventilation. Students were seated individually or in pairs at separate tables facing the chalkboard. The desks and chairs were uniformly distributed within the classrooms, with the number of rows ranging from 4 to 6 and the number of columns ranging from 3 to 7. A more detailed description is provided in Table A1 of the ESM.

2.1.2 Instrumentation, data collection, and quality assurance

Newly purchased portable PM2.5 monitors (BLATN BR-A

series, Beijing, China) were used to measure PM2.5 concentrations. The TEGONGMAO 4G Camera (Xiamen Magic Bird Technology Co., Xiamen, China) was used to capture video of children's activities in classrooms. This camera can start video capture when people are active and automatically stop when there is no activity.

To ensure the accuracy of the collected data, collocation measurements were conducted for two days (one before starting and the other after the completion of the experiment), using a research-grade instrument SDS029-FQ Multi-Channel Particle Spectrum Sensor (NOVA Technology, Shandong, China) (Wang et al. 2024a; Yuan et al. 2024). During the collocation measurements, six BLATN monitors were placed together with SDS029-FQ in controlled laboratory conditions. The SDS029-FQ was placed in the middle of the chamber, with six BLATN monitors situated around it at the same inlet height. Arizona test dust was injected into the chamber and a mixing fan was kept on during the calibration process to mix particles uniformly throughout the chamber (Ren et al. 2020). The BLATN monitors and SDS029-FQ measured the indoor PM concentration simultaneously every minute. Among all monitors used in the study, high Pearson correlation coefficients (r) were found between SDS029-FQ and BLATN monitors, with all r values exceeding 0.94. This indicates a strong agreement across all PM monitors used in the study. However, all BLATN monitors were reporting higher average PM2.5 concentrations than those measured by SDS029-FQ during the collocation study. Therefore, linear regression models were required to minimize this measurement error among BLATN monitors (Kumar et al. 2023; Kumar et al. 2024) (Text A1 and Table A2 of the ESM). The measurement errors of portable PM2.5 monitors were reduced to 3% of the concentration compared with high-end equipment.

The placement of instruments in the classroom is shown in Figure 1. The camera was fixed above the blackboard to cover the entire classroom, while the PM2.5 monitor was placed below the blackboard to minimize disruption to regular classroom order and record real-time concentration variations caused by indoor and outdoor pollutant sources. Video data were collected over approximately three weeks in autumn at both schools, while pollutant data were collected in autumn at School A and in both autumn and winter at School B.

Informed written consent was obtained from the children and their parents for the study. All children could withdraw from the study at any time. Data were gathered in compliance with the principles of the Helsinki Declaration. All experimental procedures have undergone ethical review, with the approval number 202304002.

2.2 Architecture of the proposed framework for capturing speed and duration

To estimate human movement speeds and durations, a workflow was established: (1) the experimental camera was calibrated and the captured videos were de-distorted; (2) children were detected and tracked in the video frames using the YOLO v9 and DeepSORT algorithms; (3) pixel coordinates were mapped to camera coordinates; (4) the movement speed and duration of each child in the video were calculated.

2.2.1 Part 1: Camera calibration

A wide-angle camera, which can cause inaccurate representations due to lens distortion, was used to capture the entire classroom scene (Jacobson et al. 2001). To obtain the internal reference matrix and distortion parameters, the MATLAB camera calibration toolbox based on Zhang's calibration (Zhang 2000) method was employed. Twenty images were captured at different positions by varying the spatial location of the calibration template (an 11 × 8 checkerboard with each black square measuring

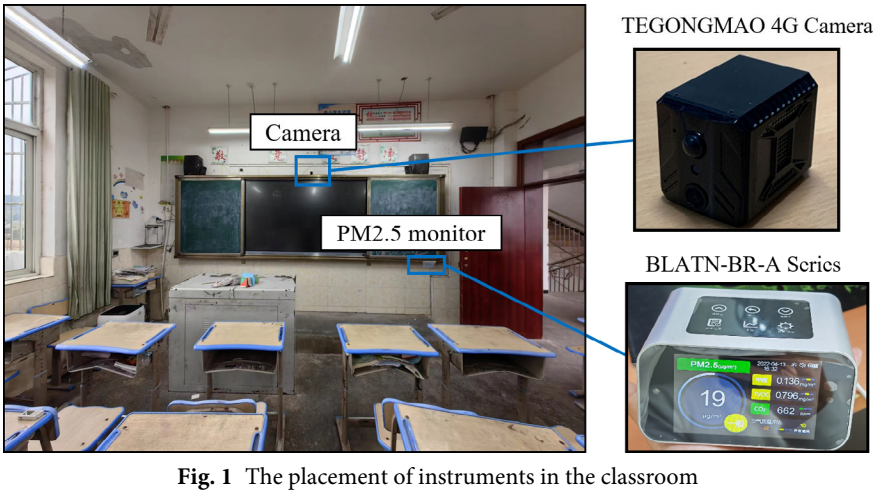

Fig. 1 The placement of instruments in the classroom

25 mm × 25 mm) while keeping the camera fixed. The camera used had a focal length of 4 mm, and the physical size of the image sensor was 1 inch. The calibration results are shown in Table A3 of the ESM.

2.2.2 *Part 2: Multi-object detection and tracking*

Over the past half-century, YOLO has evolved through multiple variants, with YOLO v9 emerging in 2024 as the latest iteration (Wang et al. 2024b). Building on YOLO v7, YOLO v9 introduces Programmable Gradient Information (PGI) to cope with the various variations required for deep networks to achieve multiple goals. It also proposes a new lightweight architecture, the Generalized Efficient Layer Aggregation Network (GELAN), based on gradient path planning. Our application is based on YOLO v9 for its precise detection capability and the DeepSORT algorithm for its adeptness in handling occlusion and distinguishing between similar objects, as described in Figure 2.

YOLO v9, with its low parameter count and computational complexity, is well-suited for dense crowd detection in resource-limited environments (Wang et al. 2022). DeepSORT utilises YOLO v9 detections to track children across video frames, using Kalman filtering for predicting target positions (Kalman 1960; Song et al. 2023) and the Hungarian algorithm for associating detections with predictions, assigning unique IDs to tracked objects (Bewley et al. 2016; Wojke et al. 2017). DeepSORT also employs a cascade matching strategy to minimize identity switches and tracking failures during occlusion (Wojke et al. 2017). These outputs enable the analysis of children's movements by estimating their coordinates, walking speed, and duration (Shirazi and Morris 2015).

2.2.3 *Part 3: Coordinate conversion in different coordinate systems*

After obtaining the pixel coordinates of each ID, the pixel coordinates converted to camera coordinates were performed based on the pinhole model and camera fixed parameters such as focal length. Figure 3 displays the schematic diagram of monocular camera ranging. By utilizing the principle of the pinhole model, as well as the pixel coordinate differences between two points and the transformation relationships

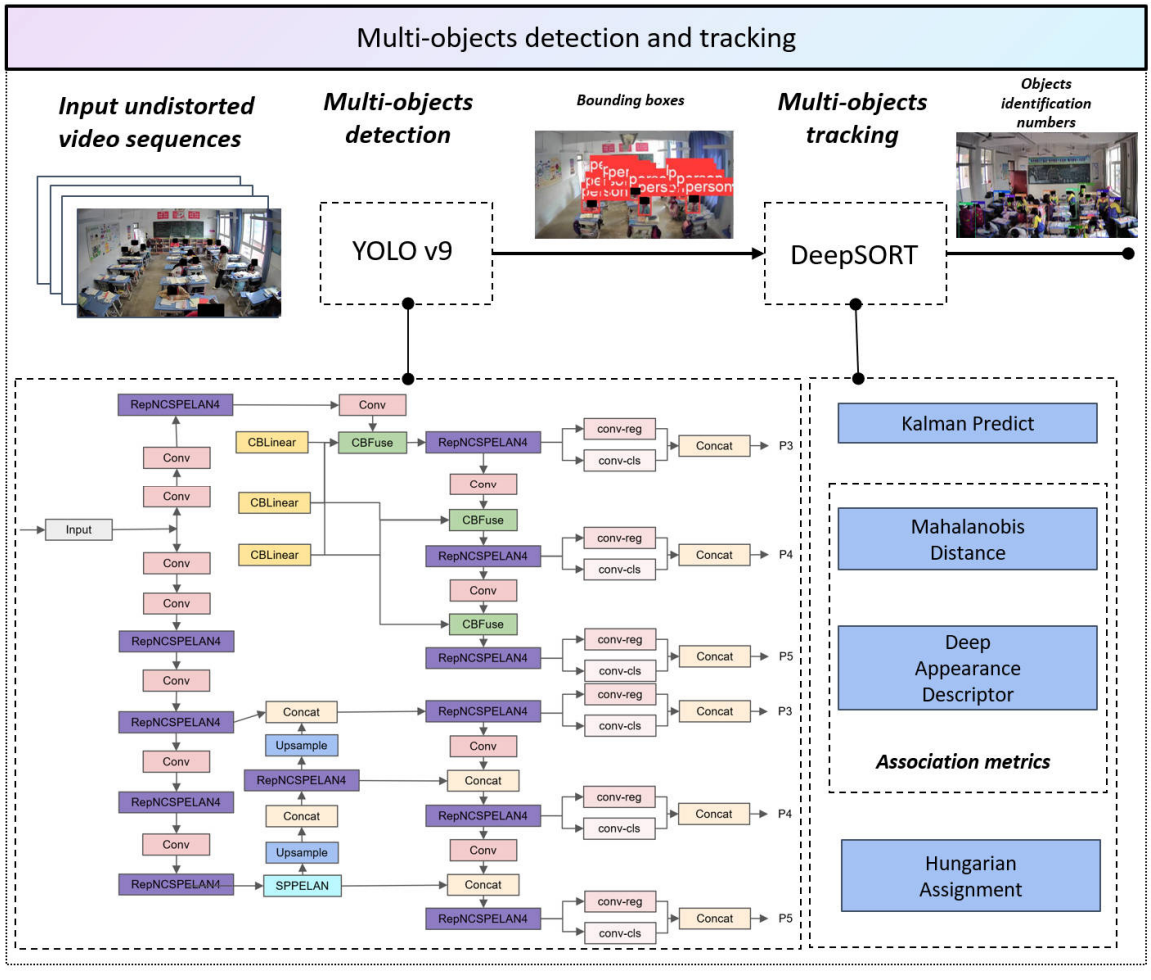

Fig. 2 The architecture of multi-object detection and tracking

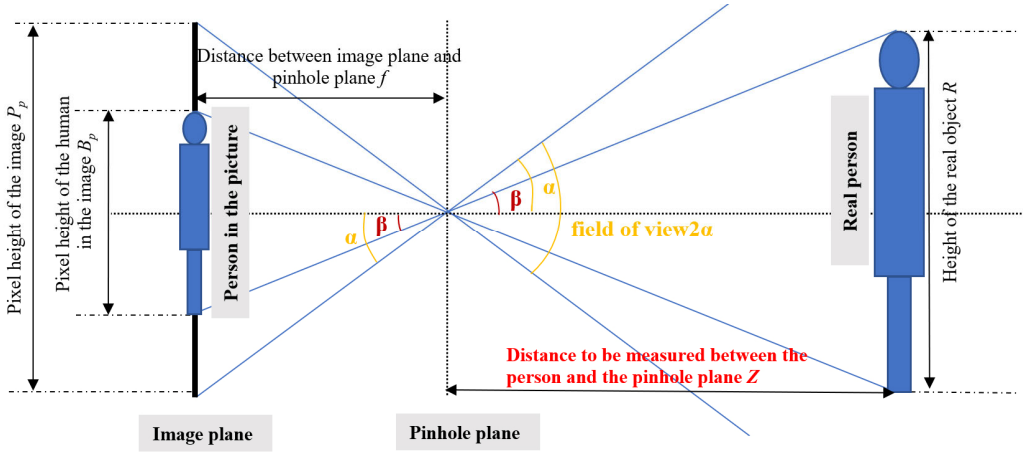

Fig. 3 Schematic diagram of pinhole model

among different coordinate systems, the real-time coordinates (X, Y, Z) of the moving children were calculated. The detailed calculation process is shown in Text A2 of the ESM.

2.2.4 *Part 4: Speed and duration calculation*

The duration and speed were calculated after obtaining the coordinates under the camera coordinate system. The coordinates data was extracted at intervals of every five frames, which can effectively prevent the omission of high-intensity activities with short duration. The number of frames in which the target appeared was recorded to calculate the duration of the activity and the average speed.

The Euclidean distance is used for the calculation of the distance dist_i between the coordinate points of the front and back frames, and the formula is as Equation (1):

$$\text{dist}_i = \sqrt{(X_i - X_{i-5})^2 + (Y_i - Y_{i-5})^2 + (Z_i - Z_{i-5})^2} \quad (1)$$

where (X_i, Y_i, Z_i) is the coordinate of the target person in frame i and (X_{i-5}, Y_{i-5}, Z_{i-5}) is the coordinate of the target person in the former target frame i–5. Speed of human instantaneous movement speed per five frames (Speed_i) can be calculated by dividing the distance by travelling time:

$$\text{Speed}_i = \frac{\text{dist}_i}{t} \quad (2)$$

where t denotes the time for every five frames (30 frames per second), equivalent to 1/6 s. Equation (2) can be used to estimate the speed of human movement between any two identified frames in m/s.

Use the average of the instantaneous speeds to define the average speed $\text{Speed}_{\text{average}}$. The calculation formula is shown in Equation (3):

$$\text{Speed}_{\text{average}} = \frac{\sum_{i=m+5}^{n} \text{Speed}_i}{\frac{n-m}{5}} \quad (3)$$

where m is the number of frames the target first appeared, and n is the number of frames the target last appeared.

The formula for calculating the duration of each activity per ID is as Equation (4):

$$\text{Duration} = \frac{n-m}{5} \cdot t \quad (4)$$

where n, m, and t take the same values as above.

2.3 Object detection, tracking, and speed estimation performance

2.3.1 *Custom dataset*

To make the YOLO v9 model more adaptable to our data, we retrained the YOLO v9 algorithm using a custom image dataset, including 200 randomly selected video screenshots from each grade, totalling 1200 screenshots. It covered every recess throughout the day. Specifically, 17,995 bounding boxes were labelled to identify the children in each screenshot. The dataset was randomly selected in the ratio of 8:1:1 and accordingly divided into training sets, validation sets, and test sets. The evaluation results of our retrained algorithm will be discussed in Section 2.3.3.

2.3.2 *Implementation environment*

The training environment is the PyCharm integrated development environment. The hardware configuration is NVIDIA GeForce RTX 3080 and 13th Gen Intel(R) Core (TM) i5-13400F with 32 GB of RAM. All code implementations were developed in Python.

2.3.3 *Evaluation results*

2.3.3.1 *Human detection and tracking*

To reasonably assess the system's performance, the detection and tracking performance was evaluated separately. Mean

Average Precision (mAP) is a widely accepted metric for evaluating object detection performance (Redmon et al. 2016; Ren et al. 2017; Zhu et al. 2020). The YOLO v9 detector had a value of 0.89 for $mAP_{0.5}$ and a value of 0.57 for $mAP_{0.5:0.95}$ on the custom dataset. These metrics are on par with the performance of existing algorithms for classrooms as well as other dense scenes (Ding et al. 2020; Chen et al. 2024), suggesting that the retrained YOLO v9 model has good overall performance in detecting the children in our collected videos.

Currently, key target-tracking performance metrics include Multiple Object Tracking Accuracy (MOTA) and Multiple Object Tracking Precision (MOTP). These metrics were evaluated using nine videos categorized by population density: three low-density videos (with 5, 10, and 15 children), three medium-density videos (with 20, 25, and 30 children), and three high-density videos (with 35, 40, and 45 children). The MOTA and MOTP values were 50.37% and 0.22, respectively. These results are comparable to those of state-of-the-art algorithms on complex datasets (Dendorfer et al. 2021; Dai et al. 2022), indicating that the DeepSORT algorithm performs well in tracking children in our collected videos.

2.3.3.2 *Speed estimation*

Mean Absolute Error (MAE), Mean Absolute Percentage Error (MAPE), and Root Mean Square Error (RMSE) are widely used to evaluate model performance errors (Yu and Gu 2019; Bell et al. 2020; Sangsuwan and Ekpanyapong 2024). For detailed explanations and calculation formulas, see Text A3 of the ESM.

To assess the performance of speed evaluation, 10 subjects were observed walking and running at three different speeds (low: 0.6 m/s, medium: 1.2 m/s, high: 1.8 m/s) in a classroom setting. Their speeds were determined by measuring distances and timing intervals, while corresponding activities were recorded and analysed using the algorithm. The resulting MAE was 0.08 m/s, RMSE was 0.09 m/s, and MAPE was 8.96%, aligning with the precision of prior research (Jiao and Fei 2023). These metrics indicate good accuracy in identifying children's activity speeds in classrooms.

3 Results and Discussion

3.1 Differences in speed distribution across years

3.1.1 *Distribution of activity speed in different age groups*

As children's chronological age increases, they undergo changes in biological, psychological, and social aspects (Eccles 1999), which are the key factors influencing children's activity patterns (Kohl and Hobbs 1998). Therefore, for data analysis, we divided the students in Years 1 to 6 into three groups according to the commonly used criteria for children's chronological age in related research (Doyle et al. 2006; Goodway et al. 2019): the lower age group (Years 1 and 2; approximately 6–7 years old; middle childhood), the middle age group (Years 3 and 4; approximately 8–9 years old; late childhood), and the upper age group (Years 5 and 6; approximately 10–11 years old; early adolescence).

Data cleansing was performed by deleting very brief activities of less than 1 s. The speed values were categorized at 0.2 m/s intervals, and the frequency distribution within each interval was calculated. Figure 4 illustrates the range of speeds and their frequency distributions across different age groups. The lower age group exhibited a slightly narrower range of speeds compared to the middle and upper age groups. This trend can be attributed to the increase in walking and running speeds with age (Papaiakovou et al. 2009; Cadieux et al. 2023). Additionally, the speed distributions for all groups were predominantly within the 0–3 m/s range.

Table A4 of the ESM presents statistics on average activity speeds by age group, including mean, median, and range. The data reveal a decreasing trend in both mean and median speeds from the lower to the upper age groups, indicating that the intensity of activity is higher in the lower age group than in the middle and upper age groups. While children's running speed increases with age (Papaiakovou

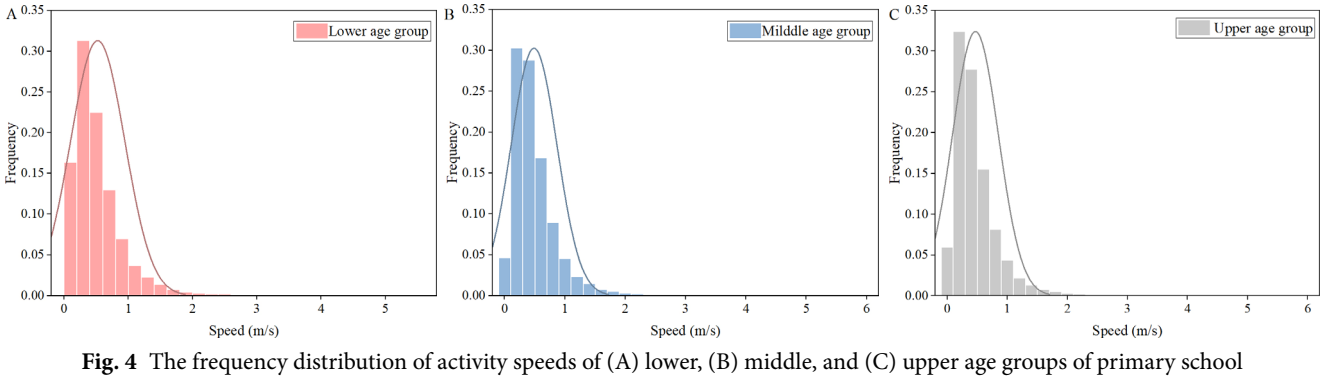

Fig. 4 The frequency distribution of activity speeds of (A) lower, (B) middle, and (C) upper age groups of primary school

et al. 2009; Cadieux et al. 2023), their subjective willingness to engage in activities may be a more significant determinant of activity intensity. Research has shown that as children grow older, they tend to shift from active play to light-intensity social activities (Ridgers et al. 2012), which may account for the observed decline in activity speeds.

3.1.2 *Statistical analysis of speed differences in different age groups*

To further clarify the differences in activity speed between age groups, statistical analysis was conducted using SPSS software. The Kolmogorov–Smirnov test indicated the activity speeds of children in all three groups ($p < 0.001$) were not normally distributed. Consequently, a nonparametric Kruskal–Wallis ANOVA test was used to examine overall differences in group distributions based on mean ranks. A p-value of less than 0.05 was considered statistically significant.

The Kruskal–Wallis ANOVA test revealed significant differences in activity speeds across the three age groups ($\chi^2(2, N = 66{,}216) = 269.34$, df = 2, $p < 0.001$), with mean ranks of 34,501.08 for the lower age group, 33,306.02 for the middle age group, and 31,562.35 for the upper age group. The activity speeds of children in the middle and upper age groups were significantly lower than those in the lower age group. Post-hoc pairwise comparisons using the Nemenyi test further indicated significant differences in speeds between the lower and middle age groups ($p < 0.001$), between the lower and upper age groups ($p < 0.001$), and between the middle and upper age groups ($p < 0.001$). These results are summarized in Table A5 of the ESM.

Combined with the median values in Table A4 of the ESM, the Nemenyi test results demonstrate a significant decline in activity speeds with increasing age. This trend may be attributed to the higher frequency of strenuous activities among younger children (Telford et al. 2005; Ridgers et al. 2012).

3.2 Distribution of physical activity intensity in different age groups

3.2.1 *Criteria for the classification of physical activity intensity*

According to the Physical Activity Guidelines for Chinese Children and Youth (Zhang et al. 2017), the intensity of activity is categorised into three levels based on Metabolic Equivalent (MET), namely light-intensity activity (1.5–2.9 MET), moderate-intensity activity (3.0–5.9 MET) and vigorous-intensity activity (≥6.0 MET). Reading, writing, and drawing are common light-intensity activities, while walking and running are typical for moderate- and vigorous-intensity activities, respectively (Zhang et al. 2017; US Department of Health and Human Services 2018).

Based on data sources recommended by the Physical Activity Guidelines for Chinese Children and Youth (Zhang et al. 2017), 1.79 m/s (with a MET value close to 6.0 for children aged 6–12 (Butte et al. 2018)) was identified as the threshold for moderate-intensity physical activity (MPA) and vigorous-intensity physical activity (VPA); 0.89 m/s (with a MET value close to 3.0 for children aged 6–12 (Butte et al. 2018)) was identified as the threshold for MPA and light-intensity physical activity (LPA).

3.2.2 *Physical activity intensity distribution based on the criteria*

Figure 5 presents the frequency distribution of activity intensity across different age groups, revealing that LPA constitutes the largest proportion for all age groups. This finding aligns with that of Pawlowski et al. (2016), who reported that LPA is most prevalent in school settings.

Compared to previous studies by Bailey et al. (1995) and Ruch et al. (2013), our study found a 7%–15% higher proportion of LPA. This discrepancy may be attributed to differences in activity space and characteristics of the Chinese education environment. Previous research has shown that children tend to be more active in spacious environments,

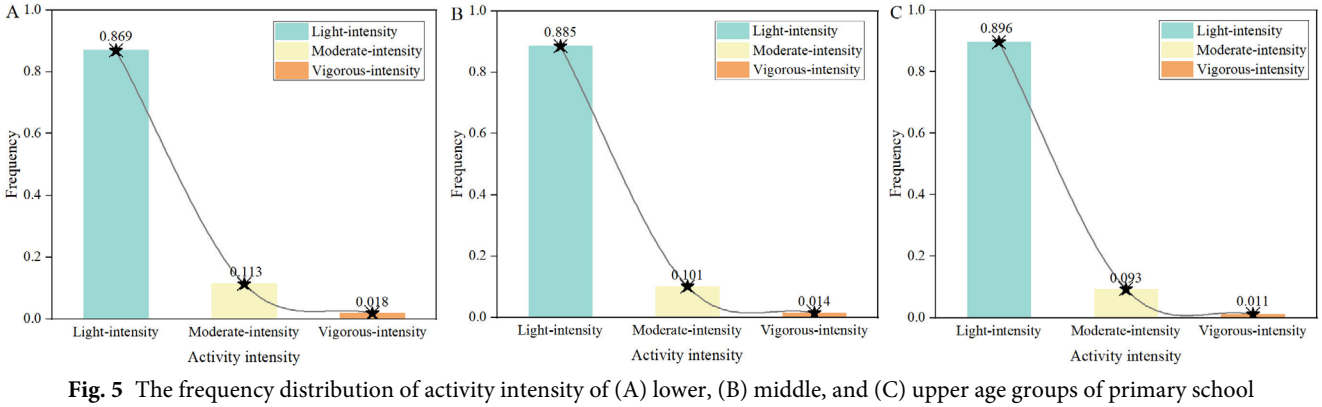

Fig. 5 The frequency distribution of activity intensity of (A) lower, (B) middle, and (C) upper age groups of primary school

with increased per capita play space correlating to higher levels of strenuous activity (Pellegrini and Smith 1993; Ridgers et al. 2010). However, in Chinese primary school classrooms, high population density and the dispersed layout of desks and chairs restrict children's movement. Additionally, the emphasis on academic success (Johns and Vertinsky 2006), safety concerns (Wang 2019; Xie et al. 2024), and the requirement for regular eye exercises during recess (Beresin 2016) further limit physical activity. These factors likely contribute to the higher proportion of LPA observed in our study. The restricted activity space within classrooms results in more scattered PM distribution due to prolonged interaction between the body and particles, leading to higher PM concentrations near the breathing zone (Tao et al. 2017a, 2017b).

For LPA, the frequencies were 0.869, 0.885, and 0.896 for the lower, middle, and upper age groups, respectively, showing an overall increasing trend. In the case of MPA, the frequencies were 0.113, 0.101, and 0.093 for the lower, middle, and upper age groups, respectively. For VPA, the frequencies were 0.018, 0.014, and 0.011, respectively. Both MPA and VPA exhibited a clear decline in frequency with increasing age. These trends align with findings by Rowlands et al. (2008), who reported that older children engage less in strenuous physical activity and more in rest or light physical activity compared to younger children. The preferences for children's activities we obtained for recess in the classroom are consistent with trends for activities in open-ended settings.

In the present study, MPA and VPA decreased by 2.0% and 0.5%, respectively, from the lower to the upper age groups. Consistent with our findings, previous research has shown that younger children tend to be more active than older children during recess (Telford et al. 2005; Ridgers et al. 2012). Specifically, each year of age increase is associated with a relative reduction in mean VPA and MPA (Telford et al. 2005; Lopes et al. 2006; Corder et al. 2016).

The lower motivation to participate in MPA and VPA among older children may be attributed to a shift in focus from active play to social behaviours with low levels of physical activity (Hardy et al. 2007). LPA, such as sit-down conversations to develop interactions with peers, have become mainstream, particularly during early adolescence (Larson and Verma 1999; Hardy et al. 2007). Additionally, in regions where education is highly valued, such as Asia, the increasing academic pressure leads adolescents to allocate more time to their studies as they grow older (Chung et al. 1993; Larson and Verma 1999).

3.2.3 Speed distribution at different activity intensities in different age groups

The statistical results of activity speed at different activity intensities in different age groups are shown in Table 1. It can be seen that as age rose, activity speeds of LPA and MPA decreased. For VPA, the activity speed decreased in the middle age group but increased in the upper age group.

The Kruskal–Wallis ANOVA test was used to perform an omnibus test on the differences in group distributions because of the non-normal distribution of activity speed. Significant differences in speed were detected across age groups for LPA ($p < 0.001$), MPA ($p = 0.011$), and VPA ($p = 0.022$). The Nemenyi test was applied to the subsequent pairwise comparisons, as presented in Table A6 of the ESM. The data revealed significant differences in activity speed between all pairs of age groups at LPA, whereas significant differences were observed only between the middle and upper age groups at MPA and VPA.

3.3 Duration of different types of children's activities

3.3.1 Distribution of activity duration in different age groups

Histograms depicting the durations of activities at different intensity levels across various age groups are presented in Figure 6. Notably, regardless of the activity intensity, the durations are consistently brief, highlighting the highly transient nature of children's classroom activities. This finding is consistent with previous studies that have emphasized the transient characteristics of children's activities (Bailey et al. 1995; Lopes et al. 2006; Rowlands et al. 2008). As illustrated in Figure 6, the range of variation in the duration of recess activities decreases gradually from LPA to VPA. This trend has also been observed in studies not restricted to classroom settings (Bailey et al. 1995; Lopes et al. 2006; Rowlands et al. 2008).

In the present study, with a data collection interval of approximately 0.17 s, over 95% of LPA lasted less than 15 s, with a median duration of 4.7 s across all age groups. 96% and 98.5% of MPA and VPA lasted less than 10 s, with

Table 1 Statistical results of activity speed at different activity intensities in different age groups

Group	Activity intensity	Mean speed (m/s)	Median speed (m/s)
Lower age group	LPA	0.39	0.36
	MPA	1.19	1.13
	VPA	2.51	2.25
Middle age group	LPA	0.38	0.35
	MPA	1.19	1.13
	VPA	2.45	2.21
Upper age group	LPA	0.36	0.32
	MPA	1.17	1.11
	VPA	2.58	2.30

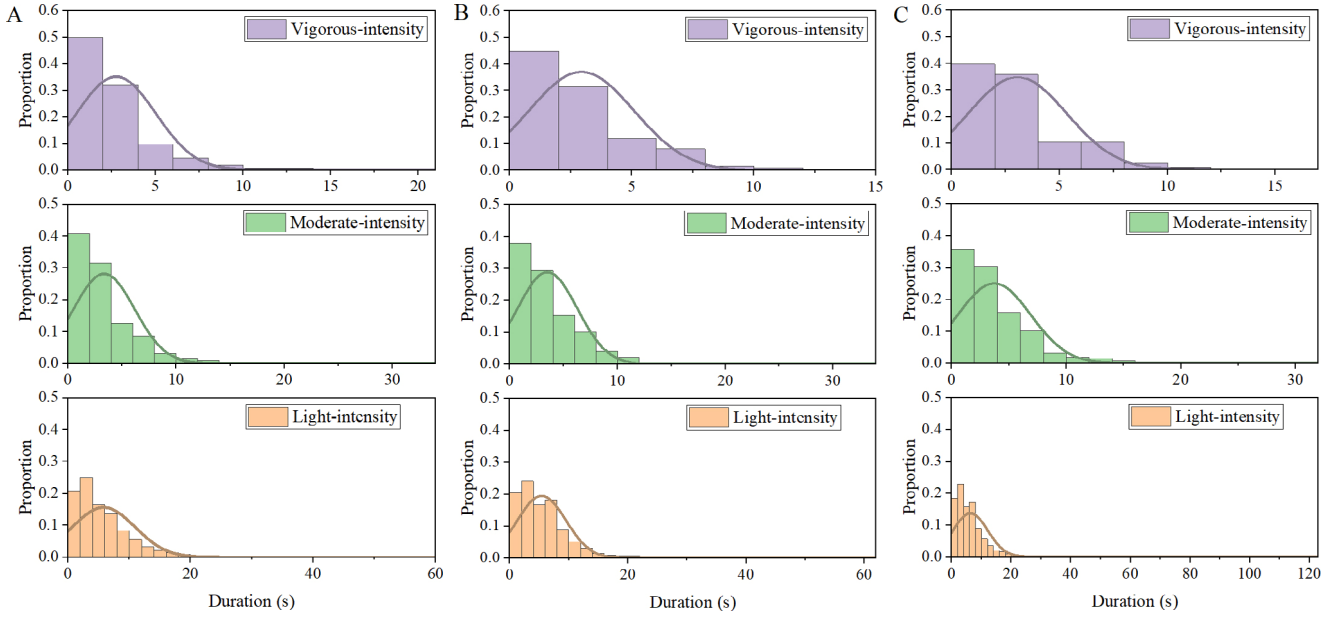

Fig. 6 Histograms of the duration of activities of different intensities in (A) lower, (B) middle, and (C) upper age groups of primary school

median durations of 2.5 and 2.2 s, respectively. Previous studies have reported that most VPA fall within the 2–10 s range (Baquet et al. 2007), and over 95% of MPA and VPA episodes last less than 15 s (Bailey et al. 1995; Lopes et al. 2006; Baquet et al. 2007). Median durations for LPA, MPA, and VPA have been reported as 4–6 s, 2–6 s, and 1–3 s, respectively (Bailey et al. 1995; Ruch et al. 2013).

The median duration of activities across all intensity levels in our study was lower than in other studies. This discrepancy may be attributed to the restricted activity space within classrooms, which limits the area available for movement and results in shorter activity durations. Additionally, the shorter data collection interval used in this study (compared to previous studies) enabled more precise identification of activity durations (Baquet et al. 2007).

3.3.2 Statistical analysis of activity duration in different age groups

The duration of different activity intensities in different age groups is shown in Figure 7. An overall increasing trend in activity duration was observed from the lower to the upper age groups for activities at all intensity levels. Additionally, a gradual decrease in duration was noted from LPA to VPA across all groups.

Differences in activity duration across age groups at various intensity levels were further analysed using Kruskal–Wallis ANOVA tests due to the non-normal distribution of activity duration. The statistical results are presented in Table 2. Significant differences in the duration of LPA and MPA were observed across the lower, middle, and upper age groups, with activity duration increasing with age. Similar findings were reported by Lopes et al. (2006), who also observed significant differences in LPA duration among children aged 6–10 years, with durations increasing with age. In contrast, the present study additionally identified significant differences in MPA duration among different age groups. This may be attributed to the shorter data collection epoch used in this study compared to previous

Table 2 Statistical results of duration in different activity intensities of different age groups

Activity intensity	Median duration (s)			Kruskal Wallis-*H*	*p*-value
LPA	Lower age group	Middle age group	Upper age group	150.611	**<0.001**
	4.33	4.50	5.00		
MPA	Lower age group	Middle age group	Upper age group	19.815	**<0.001**
	2.33	2.50	2.67		
VPA	Lower age group	Middle age group	Upper age group	3.724	0.155
	1.92	2.16	2.33		

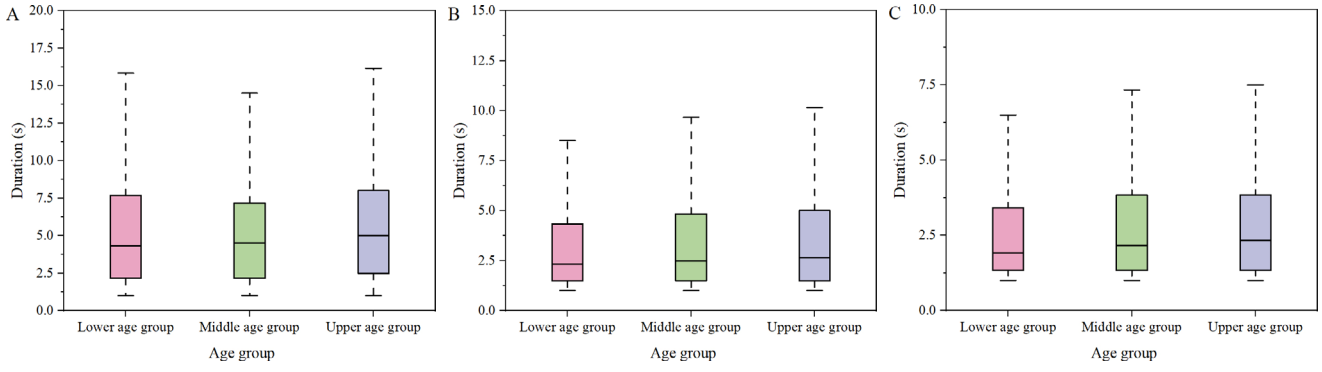

Fig. 7 Duration distribution of different age groups in (A) light, (B) moderate, and (C) vigorous intensity activities

research, which better distinguishes lower-intensity activities from higher-intensity activities (Ridgers et al. 2005).

Following the Kruskal–Wallis test, the results of pairwise comparisons using the Nemenyi test are presented in Table A7 of the ESM. For LPA, the duration was significantly longer in the upper age group compared to the middle and lower age groups. This phenomenon may be because older children face academic pressures and devote more time to LPA of sedentary learning (Chung et al. 1993; Larson and Verma 1999). For MPA, children in the lower age group spent significantly less time compared to the other two groups, likely because younger children tend to engage in physical activities for shorter durations (Obeid et al. 2011).

3.4 Assessment of PM2.5 inhalation dose during recess activities for children in different age groups

3.4.1 Distribution of PM2.5 concentration in different age groups

Figure 8 illustrates the detailed distribution of PM2.5 concentrations across different age groups and seasons during recess. The overall concentration range decreased from the lower to the upper age groups. This trend aligns with previous studies reporting higher PM concentrations in classrooms of younger children compared to other age groups (Fromme et al. 2007; Alves et al. 2013). Children in the lower age groups exhibit higher activity intensity, which likely contributes to the elevated PM levels observed in their classrooms.

Indoor PM concentrations are significantly higher in winter than in autumn. Specifically, the average PM concentrations for the lower, middle, and upper age groups in autumn were 54.08, 51.70, and 49.88 μg/m^3, respectively. During the non-heating season, windows are primarily kept open, leading to a higher air change rate and consequently lower indoor PM concentrations. In contrast, the average PM concentrations for the lower, middle, and upper age groups during winter were 183.02, 177.42, and 174.57 μg/m^3, respectively. This disparity may be attributed to inadequate ventilation rates and higher outdoor PM2.5 concentrations.

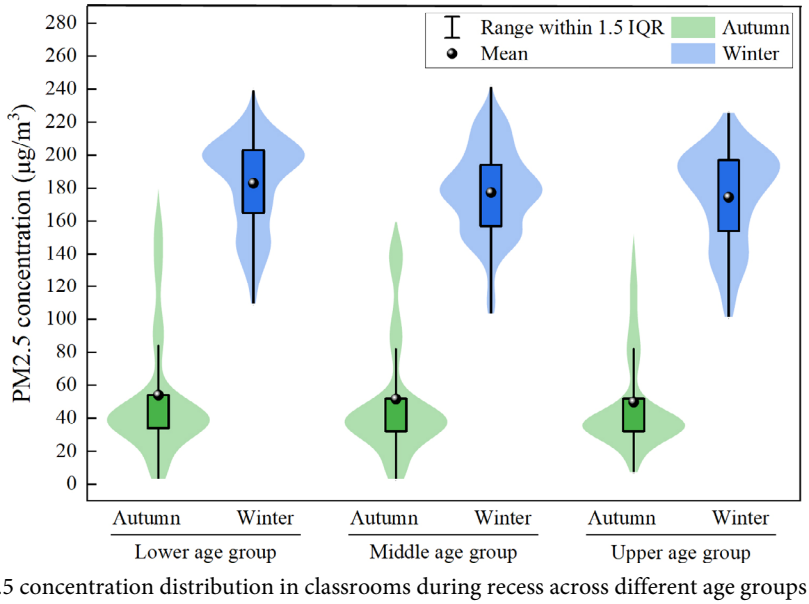

Fig. 8 PM2.5 concentration distribution in classrooms during recess across different age groups and seasons

A few higher concentrations, even reaching about 180 μg/m³ in autumn and 240 μg/m³ in winter. The higher values were found in the morning when children entered the school, at the end of the school day, and during the recess exercise period. These peaks are attributed to children's intensive activities, which cause the resuspension of settled particles from daily tasks, skin shedding, and clothing (Fromme et al. 2007; Licina et al. 2017; Yuan et al. 2023). Children arriving at and leaving school in large numbers drive PM2.5 concentrations to peak during these periods (Yang et al. 2023; Zhou et al. 2021). Similarly, as children leave the classroom for activities during recess, their high activity levels lead to elevated PM2.5 concentrations.

3.4.2 The effects of outdoor PM2.5 and children's activity patterns on indoor PM2.5 concentrations

In school classrooms, indoor PM concentrations are primarily determined by surrounding air pollution levels and occupant activity types (Majd et al. 2019; Son 2023). To investigate this relationship, we included outdoor PM2.5 concentration, activity speed, and duration as influencing factors. Data collected over a single day from each classroom, with average activity speed, duration, and indoor/outdoor PM2.5 concentrations calculated per minute, generated a dataset comprising 1,416 records. Multiple linear regression models were then constructed to identify the relationship between indoor PM2.5 concentrations and these factors. Prior to analysis, collinearity was assessed using variance inflation factors (VIF), with values ranging from 1.024 to 1.132, all below 10, indicating no multicollinearity among the independent variables (Ul-Saufie et al. 2011).

Table 3 presents the parameters derived from the multiple regression analysis for outdoor PM2.5, speed, and duration. As expected, outdoor PM2.5 and children's activity speed were strongly associated with elevated indoor PM2.5 concentrations. Specifically, a 1 μg/m³ increase in outdoor PM2.5 corresponded to a 0.528 μg/m³ increase in indoor PM2.5 ($p < 0.001$), while a 1 m/s increase in speed resulted in a 15.197 μg/m³ increase in indoor PM2.5 ($p < 0.001$). Conversely, children's activity duration was significantly associated with lower indoor PM2.5 concentrations, with a 1 s increase in duration corresponding to a 0.658 μg/m³ decrease in indoor PM2.5 ($p = 0.002$). This may be attributed to the fact that longer durations are generally associated with lower activity speeds.

Table 3 Multivariate analysis of predictors of indoor PM2.5 concentrations

Influencing factor	Coefficient	95% Confidence interval	*p*-value	R^2
Outdoor PM2.5 (per μg/m³)	0.528	0.495, 0.561	<0.001	0.525
Speed (per m/s)	15.197	12.518, 17.875	<0.001	
Duration (per second)	−0.658	−1.078, −0.238	0.002	

3.4.3 PM2.5 inhalation dose calculation and feasible improvement measures

According to the previously described methodology for the calculation of inhalation dose (D) (Slezakova et al. 2018; Slezakova et al. 2019; Slezakova et al. 2020), D in this study was calculated as Equation (5):

$$\mathrm{Dose}(D) = \sum_{i=1}^{3} (\mathrm{BR}_{\mathrm{intens}_i} / \mathrm{BW}) \times C \times T_{\mathrm{intens}_i} \tag{5}$$

where D is the age-group-specific dose (μg/kg); intens represents the activity intensity; the values 1, 2, and 3 for i represent LPA, MPA, and VPA, respectively; $\mathrm{BR}_{\mathrm{intens}_i}$ represents the age-group-specific breathing rate at different activity intensities (m³/min); BW is the age-group-specific body weight (kg); C is the average PM concentration in the classroom (μg/m³); T_{intens_i} is the exposure time for different activity intensities per day (min).

The values of $\mathrm{BR}_{\mathrm{intens}_i}$ were determined based on the data from the Chinese Exposure Factors Handbook (Duan 2016). The values for BW were retrieved from the data in the standard GB/T26158-2010 Human Dimensions of Chinese Minor (GB 2010).

Different intensity activities have varying probabilities and durations. Based on this, the T_{intens_i} was calculated by Equations (6) to (7):

$$p_{\mathrm{intens}_i} = \frac{P_{\mathrm{intens}_i} \times \mathrm{Duration}_{\mathrm{intens}_i}}{\sum_{i=1}^{3} \left(P_{\mathrm{intens}_i} \times \mathrm{Duration}_{\mathrm{intens}_i} \right)} \tag{6}$$

$$T_{\mathrm{intens}_i} = p_{\mathrm{intens}_i} \times T_{\mathrm{total}} \tag{7}$$

where P_{intens_i} is the probability proportion of different activity intensities; p_{intens_i} is the time proportion of different activity intensities; $\mathrm{Duration}_{\mathrm{intens}_i}$ is the activity duration of different intensities; T_{total} is the total time of PM exposure per day (min). The values of P_{intens_i} were derived from the information provided in Section 3.2.2. $\mathrm{Duration}_{\mathrm{intens}_i}$ was obtained from Table 2. T_{total} was determined based on the timetable of the two selected primary schools (120 min). Table 4 shows the values of each parameter and the PM2.5 inhalation dose calculation for all age groups.

As can be seen from Table 4, the PM2.5 inhalation doses vary among different age groups. The variability in PM2.5 inhalation doses between different groups was defined by Equation (8):

$$\text{Relative Difference} = \left| \frac{D_{\text{age-group}_i} - D_{\text{age-group}_j}}{D_{\text{age-group}_j}} \right| \times 100\% \tag{8}$$

where *i* and *j* represent different age groups, the age groups defined by *i* and *j* must not be the same in each calculation.

The inhalation doses in each age group and the relative differences are shown in Table A8 of the ESM. It can be observed that the higher indoor PM concentrations in winter resulted in children's daily inhalation dose being 3.38 to 3.50 times higher than that in autumn. Additionally, the inhalation dose decreased with increasing age, with the lower age group having the highest daily inhalation dose. Compared to the lower age group, the inhalation dose decreased by 14.67% in the middle age group and by 30.64% in the upper age group. Furthermore, the inhalation dose of the upper age group was 18.72% lower than that of the middle age group.

Children, as one of the susceptible groups, are more vulnerable to the health impacts of PM. For instance, an increase in the average daily inhalation dose of PM2.5 was associated with decreased lung function (Li et al. 2020). Given these findings, it is imperative to develop air pollution management policies that prioritize susceptible populations, particularly younger children.

Higher PM2.5 concentrations during recess are a significant cause of increased inhalation dose. Therefore, in primary school classrooms, especially those with younger children who have higher activity levels, relevant departments should encourage schools to proactively install air purification equipment to effectively reduce children's inhaled dose of PM2.5. In regions that cannot afford air purification equipment, optimizing classroom layouts—such as adopting a U-shaped arrangement—can effectively reduce PM2.5 concentrations, particularly in the breathing zone of elementary students (Tikul et al. 2022). Additionally, when outdoor PM2.5 concentrations are low, opening doors and windows can help dilute indoor PM2.5 levels. Moreover,

Table 4 Values of each parameter for different age groups

Age group	Parameter					Dose (μg/kg)
Lower age group	[a]BR_{intens_i} (m^3/min)	Intensity level			Value	**2.42** (autumn) **8.18** (winter)
		1			7.70E−03	
		2			1.55E−02	
		3			3.86E−02	
	[b]BW (kg)	22.7				
	C (μg/m^3)	54.08 (autumn) 183.02 (winter)				
	p_{intens_i}	Intensity level	P_{intens_i}	$Duration_{intens_i}$	Value	
		1	0.869	4.33	0.927	
		2	0.113	2.33	0.065	
		3	0.018	1.92	0.008	
	T_{intens_i} (min)	Intensity level			Value	
		1			111.24	
		2			7.80	
		3			0.96	
	T_{total} (min)	120				
Middle age group	[a]BR_{intens_i} (m^3/min)	Intensity level			Value	**2.05** (autumn) **7.03** (winter)
		1			8.20E−03	
		2			1.65E−02	
		3			4.11E−02	
	[b]BW (kg)	27.0				
	C (μg/m^3)	51.70 (autumn) 177.42 (winter)				
	p_{intens_i}	Intensity level	P_{intens_i}	$Duration_{intens_i}$	Value	
		1	0.885	4.5	0.934	
		2	0.101	2.5	0.059	
		3	0.014	2.16	0.007	
	T_{intens_i} (min)	Intensity level			Value	
		1			112.08	
		2			7.08	
		3			0.84	
	T_{total} (min)	120				

Table 4 Values of each parameter for different age groups (Continued)

Age group	Parameter					Dose (μg/kg)
Upper age group	[a]BR_{intens_i} (m^3/min)	Intensity level			Value	**1.65** (autumn) **5.77** (winter)
		1			9.70E−03	
		2			1.93E−02	
		3			4.83E−02	
	[b]BW (kg)	37.9				
	C (μg/m^3)	49.88 (autumn) 174.57 (winter)				
	p_{intens_i}	Intensity level	P_{intens_i}	$Duration_{intens_i}$	Value	
		1	0.896	5	0.942	
		2	0.093	2.67	0.052	
		3	0.011	2.33	0.006	
	T_{intens_i} (min)	Intensity level			Value	
		1			113.04	
		2			6.24	
		3			0.72	
	T_{total} (min)	120				

[a] The values for the lower age group were based on the mean breathing rates of the age groups of 5–6 years old and 6–9 years old, respectively; the values for the middle and upper age groups were based on the mean breathing rates for the age groups of 6–9 and 9–12 years old, respectively.

[b] The values for the lower age group were based on the average weights of boys and girls aged 4–6 and 7–10, respectively; the values for the middle age group and the upper age group were the average weights of boys and girls aged 7–10 and 11–12, respectively.

resuspension caused by children's indoor activities also contributes significantly to elevated indoor PM concentrations. Therefore, increasing the frequency of cleaning is an effective measure to reduce PM resuspension at the source.

4 Implication and limitation

Children's higher activity intensity compared to teenagers and young adults contributes to elevated PM concentrations in classrooms during recess (Livingstone et al. 2003; Sigmund et al. 2007). However, most previous studies have typically focused on comparing exposure concentrations in schools of different locations and analysing the contributions of various factors (Branco et al. 2019; Villanueva et al. 2021; Zhu et al. 2021), which cannot quantify children's activity patterns (speed, duration) in classrooms across different age groups. This study, leveraging machine learning algorithms and video data, quantified the key parameters of activity patterns for primary school children in different age groups. Its findings are applicable to densely populated classrooms in other regions or countries with similar layouts and education environments, such as Republic of Korea and Japan (Li et al. 2017; Kim et al. 2024). For classrooms with lower population densities and larger activity areas, the applicability of the results of this study requires further confirmation. This study offers a scientific foundation for the development of targeted strategies to mitigate indoor air pollution in educational facilities, thereby safeguarding children's health.

Nowadays, PM pollution in primary schools in China remains relatively severe (Zhu et al. 2021), and common in other developing countries (Shaddick et al. 2020). It is crucial to quantitatively describe the PM inhalation dose and its differences across different age groups in classrooms, especially considering the varying activity patterns of children in different age groups, to provide more information for policymakers and the academic community. This study synchronously collected activity data and environmental parameters and analysed the causal relationship between indoor and outdoor influencing factors and indoor PM concentrations. Additionally, this study presents a new method for quantifying children's inhalation doses based on activity patterns and environmental parameters. This method estimates and assesses the differences in PM2.5 inhalation doses among children of different age groups under varying activity patterns, emphasizing the significant contributions of activity speed, duration, and outdoor PM levels. This method is considered to provide meaningful outcomes and a methodological framework for future studies on estimating PM inhalation doses and risk assessments for children of other age groups or in other environments.

However, there are still some limitations that should be noted. Firstly, field measurements were challenging due to the study subjects being children, which restricted the investigation to two schools and yielded a limited sample size. Accordingly, this study did not encompass the variability in classroom cleaning frequencies and layouts. Secondly, due to the significant challenges associated with simultaneously and accurately obtaining parameters such as weight, gender, and activity patterns using machine learning algorithms, this study examined the influence of chronological age on activity patterns but did not account for the effects of other factors, such as weight and gender. Finally, due to the limitations of the machine learning algorithms employed in this study and the camera perspectives, partial trajectory loss occurs in a few rare blind spots and extremely crowded scenarios. In the future, it is necessary to optimize the algorithms, such as conducting multi-scale feature fusion and optimization or incorporating attention mechanisms, to improve detection accuracy and enable accurate tracking of occluded children. Moreover, multi-camera configurations or strategic planning of camera placement and field of view can effectively reduce the likelihood of trajectory loss in complex scenes. Building on these advancements, future research should be directed towards more accurately assessing the PM inhalation dose and the associated health risks.

5 Conclusions

This study employs an interdisciplinary approach to investigate children's recess activity patterns and PM2.5 inhalation doses across different age groups in primary school classrooms. The main conclusions are:

(1) A feasibility framework has been developed to utilize de-distorted video data from low-cost cameras for the detection and tracking of children in videos. The results demonstrate that the framework effectively estimates children's activity speeds and durations using low-cost cameras, thereby reducing labour-intensive demands for manual observation and data processing, as well as high costs.

(2) Children's classroom activities are predominantly low intensity, with LPA comprising the highest proportion across all age groups (ranging from 0.869 to 0.896). This LPA proportion was 7%–15% higher than that reported in previous studies, likely due to high occupant density, limited activity space, and characteristics of the Chinese education environment. Additionally, LPA increased while MPA to VPA decreased with age, possibly due to changing activity preferences and schoolwork pressures.

(3) Children's classroom activities exhibit a highly transitory nature, with median durations of recess activities decreasing from LPA (4.7 s) to MPA (2.5 s) and VPA

(2.2 s). These values are lower than those in previous studies, likely due to limited activity space and shorter sampling intervals. Significant differences in the duration of LPA and MPA were observed across the lower, middle, and upper age groups, with activity duration increasing with age.

(4) Children's activity speed, duration, and outdoor PM2.5 were strongly associated with variations in indoor PM2.5 concentrations. A 1 μg/m³ increase in outdoor PM2.5 results in a 0.528 μg/m³ increase in indoor PM2.5 ($p < 0.001$), a 1 m/s increase in activity speed leads to a 15.197 μg/m³ increase in indoor PM2.5 ($p < 0.001$), and a 1 s increase in duration reduces indoor PM2.5 by 0.658 μg/m³ ($p = 0.002$).

(5) A new method has been developed to quantify the contribution of activity patterns to PM inhalation dose and inequity between different age groups. The findings revealed that the daily inhalation dose decreased with increasing age, being 14.67% lower in the middle age group and 30.64% lower in the upper age group compared to the lower age group, indicating a higher health risk for younger children.

The findings obtained in this study offered valuable insights for offering more accurate PM-related health risk evaluation and developing air quality enhancement strategies for classrooms across various age groups in the future.

Electronic Supplementary Material (ESM): Supplementary material is available in the online version of this article at https://doi.org/10.1007/s12273-025-1295-x.

Acknowledgements

This work was supported by the National Natural Science Foundation of China (Grant No. 52278090), Ministry of Science and Technology of the People's Republic of China. Prashant Kumar acknowledges the support received through the EPSRC-funded COTRACE/SAMHE project (EP/W001411/1).

Declaration of competing interest

The authors have no competing interests to declare that are relevant to the content of this article.

Author contribution statement

All authors contributed to the study conception and design. Investigation was performed by Feng Yuan and Ziyu Shu. Formal analysis was performed by Feng Yuan, Runming Yao, Prashant Kumar, Christopher Pain, and Ziyu Shu. Funding acquisition was performed by Baizhan Li and Runming Yao. The first draft of the manuscript was written by Feng Yuan and all authors commented on previous versions of the manuscript. All authors read and approved the final manuscript.

References

Alves C, Nunes T, Silva J, et al. (2013). Comfort parameters and particulate matter (PM10 and PM2.5) in school classrooms and outdoor air. *Aerosol and Air Quality Research*, 13: 1521–1535.

Azhar MIH, Zaman FHK, Tahir NM, et al. (2020). People tracking system using DeepSORT. In: Proceedings of the 10th IEEE International Conference on Control System, Computing and Engineering, Penang, Malaysia, pp. 137–141.

Bailey RC, Olson J, Pepper SL, et al. (1995). The level and tempo of children's physical activities: An observational study. *Medicine and Science in Sports and Exercise*, 27: 1033–1041.

Baquet G, Stratton G, Van Praagh E, et al. (2007). Improving physical activity assessment in prepubertal children with high-frequency accelerometry monitoring: A methodological issue. *Preventive Medicine*, 44: 143–147.

Bell D, Xiao W, James P (2020). Accurate vehicle speed estimation from monocular camera footage. *ISPRS Annals of the Photogrammetry, Remote Sensing and Spatial Information Sciences*, V-2-2020: 419–426.

Beresin A (2016). Playing with time: Towards a global survey of recess practices. *International Journal of Play*, 5: 159–165.

Bewley A, Ge Z, Ott L, et al. (2016). Simple online and realtime tracking. In: Proceedings of the 2016 IEEE International Conference on Image Processing, Phoenix, AZ, USA, pp. 3464–3468.

Boulbair A, Benabed A, Janssens B, et al. (2022). Numerical study of the human walking-induced fine particles resuspension. *Building and Environment*, 216: 109050.

Branco PTBS, Alvim-Ferraz MCM, Martins FG, et al. (2019). Quantifying indoor air quality determinants in urban and rural nursery and primary schools. *Environmental Research*, 176: 108534.

Butte NF, Watson KB, Ridley K, et al. (2018). A youth compendium of physical activities: Activity codes and metabolic intensities. *Medicine and Science in Sports and Exercise*, 50: 246–256.

Cadieux JM, Pyhala SL, Johnson JV (2023). Pediatric walking speed normal reference values in a local population. *Pediatric Physical Therapy*, 35: 314–320.

Chen T, Chen J, Gao T, et al. (2024). A novel scene-aware pedestrian detection in dense scenes. In: Proceedings of the 2024 27th International Conference on Computer Supported Cooperative Work in Design, Tianjin, China, pp. 1316–1321.

Chinapaw MJ, Wang X, Andersen LB, et al. (2019). From total volume to sequence maps: Sophisticated accelerometer data analysis. *Medicine and Science in Sports and Exercise*, 51: 814–820.

Chung B, Kim H, Lee S, et al. (1993). Restoring Korean Education from the Bandage of Entrance Examination Education. Seoul: Nanam Publication.

Cohen Hubal EA, Sheldon LS, Burke JM, et al. (2000). Children's exposure assessment: A review of factors influencing children's exposure, and the data available to characterize and assess that exposure. *Environmental Health Perspectives*, 108: 475–486.

Corder K, Sharp SJ, Atkin AJ, et al. (2016). Age-related patterns of vigorous-intensity physical activity in youth: The international children's accelerometry database. *Preventive Medicine Reports*, 4: 17–22.

Cristani M, Raghavendra R, Del Bue A, et al. (2013). Human behavior analysis in video surveillance: A Social Signal Processing perspective. *Neurocomputing*, 100: 86–97.

Dai Y, Hu Z, Zhang S, et al. (2022). A survey of detection-based video multi-object tracking. *Displays*, 75: 102317.

De Baere S, Seghers J, Philippaerts R, et al. (2015). Intensity- and domain-specific levels of physical activity and sedentary behavior in 10- to 14-year-old children. *Journal of Physical Activity & Health*, 12: 1543–1550.

Dendorfer P, Ošep A, Milan A, et al. (2021). MOTChallenge: A benchmark for single-camera multiple target tracking. *International Journal of Computer Vision*, 129: 845–881.

Diapouli E, Chaloulakou A, Spyrellis N (2007). Indoor and outdoor particulate matter concentrations at schools in the Athens area. *Indoor and Built Environment*, 16: 55–61.

Ding J, Xu L, Guo J, et al. (2020). Human detection in dense scene of classrooms. In: Proceedings of the 2020 IEEE International Conference on Image Processing, Abu Dhabi, United Arab Emirates, pp. 618-622.

Doyle LW, Anderson P, Callanan C, et al. (2006). Respiratory function at age 8–9 years in extremely low birthweight/very preterm children born in Victoria in 1991–1992. *Pediatric Pulmonology*, 41: 570–576.

Du W, Cui Z, Wang J, et al. (2024). Quantifying the contribution of activity patterns to $PM_{2.5}$ exposure inequity between urban and rural residents by a novel method. *Building Simulation*, 17: 1323–1333.

Duan X (2016). Highlights of the Chinese Exposure Factors Handbook (Children). China Environment Publishing Group.

Eccles JS (1999). The development of children ages 6 to 14. *The Future of Children*, 9: 30–44.

Fromme H, Twardella D, Dietrich S, et al. (2007). Particulate matter in the indoor air of classrooms—Exploratory results from Munich and surrounding area. *Atmospheric Environment*, 41: 854–866.

GB (2010). GB/T 26158-2010: Human dimensions of Chinese minor. Standard Press of China.

Ghomashchi H, Paterson J, Novak AC, et al. (2024). Estimating pedestrian walking speed at street crossings using the YOLOv4 and deep SORT algorithms: Proof of principle. *Applied Ergonomics*, 119: 104292.

Goodway JD, Ozmun JC, Gallahue DL (2019). Understanding Motor Development: Infants, Children, Adolescents, Adults. Burlington, USA: Jones & Bartlett Learning.

Gu Y, Kim J, Ma J, et al. (2024). Isotemporal substitution of accelerometer-derived sedentary behavior and physical activity on physical fitness in young children. *Scientific Reports*, 14: 13544.

Hardy LL, Bass SL, Booth ML (2007). Changes in sedentary behavior among adolescent girls: A 2.5-year prospective cohort study. *Journal of Adolescent Health*, 40: 158–165.

Jacobson RE, Axford N, Ray S, et al. (2001). Manual of Photography: Photographic and Digital Imaging. Focal Press.

Jiao D, Fei T (2023). Pedestrian walking speed monitoring at street scale by an in-flight drone. *PeerJ Computer Science*, 9: e1226.

Johns D, Vertinsky P (2006). The influence of physical, cultural and social environments on health-related activity. In: Physical Activity and Health of Hong Kong Youth. The Chinese University of Hong Kong Press. pp. 182–196.

Kalman RE (1960). A new approach to linear filtering and prediction problems. *Journal of Basic Engineering*, 82: 35–45.

Kim J, Park S, Kim H, et al. (2019). Emission characterization of size-resolved particles in a pre-school classroom in relation to children's activities. *Indoor and Built Environment*, 28: 659–676.

Kim S, Kang K, Park D, et al. (2024). Assessment of $PM_{2.5}$ penetration based on airflow paths in Korean classrooms. *Building and Environment*, 248: 111103.

Kohl HW III, Hobbs KE (1998). Development of physical activity behaviors among children and adolescents. *Pediatrics*, 101: 549–554.

Kumar P, Rawat N, Tiwari A (2023). Micro-characteristics of a naturally ventilated classroom air quality under varying air purifier placements. *Environmental Research*, 217: 114849.

Kumar P, Hama S, Abbass RA, et al. (2024). Environmental quality in sixty primary and secondary school classrooms in London. *Journal of Building Engineering*, 91: 109549.

Larson RW, Verma S (1999). How children and adolescents spend time across the world: Work, play, and developmental opportunities. *Psychological Bulletin*, 125: 701–736.

Li H, Martin AJ, Yeung WJ (2017). Academic risk and resilience for children and young people in Asia. *Educational Psychology*, 37: 921–929.

Li S, Cao S, Duan X, et al. (2020). Long-term exposure to $PM_{2.5}$ and children's lung function: A dose-based association analysis. *Journal of Thoracic Disease*, 12: 6379–6395.

Li Z, Ding Y, Wang D, et al. (2023). Understanding the time-activity pattern to improve the measurement of personal exposure: An

exploratory and experimental research. *Environmental Pollution*, 334: 122131.

Licina D, Tian Y, Nazaroff WW (2017). Emission rates and the personal cloud effect associated with particle release from the perihuman environment. *Indoor Air*, 27: 791–802.

Livingstone MBE, Robson PJ, Wallace JMW, et al. (2003). How active are we? Levels of routine physical activity in children and adults. *Proceedings of the Nutrition Society*, 62: 681–701.

Lopes VP, Vasques C, Pereira B, et al. (2006). Physical activity patterns during school recess: A study in children 6 to 10 years old. *International Electronic Journal of Health Education*, 9: 192–201. Available at http://bibliotecadigital.ipb.pt/handle/10198/226.

Madureira J, Paciência I, de Oliveira Fernandes E (2012). Levels and indoor–outdoor relationships of size-specific particulate matter in naturally ventilated Portuguese schools. *Journal of Toxicology and Environmental Health*, *Part A*, 75: 1423–1436.

Majd E, McCormack M, Davis M, et al. (2019). Indoor air quality in inner-city schools and its associations with building characteristics and environmental factors. *Environmental Research*, 170: 83–91.

Obeid J, Nguyen T, Gabel L, et al. (2011). Physical activity in Ontario preschoolers: Prevalence and measurement issues. *Physiologie Appliquee*, *Nutrition et Metabolisme*, 36: 291–297.

Oliveira M, Slezakova K, Delerue-Matos C, et al. (2019). Children environmental exposure to particulate matter and polycyclic aromatic hydrocarbons and biomonitoring in school environments: A review on indoor and outdoor exposure levels, major sources and health impacts. *Environment International*, 124: 180–204.

Papaiakovou G, Giannakos A, Michailidis C, et al. (2009). The effect of chronological age and gender on the development of sprint performance during childhood and puberty. *Journal of Strength and Conditioning Research*, 23: 2568–2573.

Pawlowski CS, Andersen HB, Troelsen J, et al. (2016). Children's physical activity behavior during school recess: A pilot study using GPS, accelerometer, participant observation, and go-along interview. *PLoS One*, 11: e0148786.

Pellegrini AD, Smith PK (1993). School recess: Implications for education and development. *Review of Educational Research*, 63: 51–67.

Punn NS, Sonbhadra SK, Agarwal S, et al. (2021). Monitoring COVID-19 social distancing with person detection and tracking via fine-tuned YOLO v3 and Deepsort techniques. arXiv Preprint. Available at https://arxiv.org/abs/2005.01385.

Redmon J, Divvala S, Girshick R, et al. (2016). You only look once: Unified, real-time object detection. In: Proceedings of the 2016 IEEE Conference on Computer Vision and Pattern Recognition, Las Vegas, NV, USA, pp. 779–788.

Ren S, He K, Girshick R, et al. (2017). Faster R-CNN: Towards real-time object detection with region proposal networks. *IEEE Transactions on Pattern Analysis and Machine Intelligence*, 39: 1137–1149.

Ren J, Wade M, Corsi RL, et al. (2020). Particulate matter in mechanically ventilated high school classrooms. *Building and Environment*, 184: 106986.

Ridgers ND, Stratton G, Fairclough SJ (2005). Assessing physical activity during recess using accelerometry. *Preventive Medicine*, 41: 102–107.

Ridgers ND, Fairclough SJ, Stratton G (2010). Variables associated with children's physical activity levels during recess: The A-CLASS project. *International Journal of Behavioral Nutrition and Physical Activity*, 7: 74.

Ridgers ND, Timperio A, Crawford D, et al. (2012). Five-year changes in school recess and lunchtime and the contribution to children's daily physical activity. *British Journal of Sports Medicine*, 46: 741–746.

Rowlands AV, Eston RG (2007). The measurement and interpretation of children's physical activity. *Journal of Sports Science & Medicine*, 6: 270–276.

Rowlands AV, Pilgrim EL, Eston RG (2008). Patterns of habitual activity across weekdays and weekend days in 9–11-year-old children. *Preventive Medicine*, 46: 317–324.

Ruch N, Melzer K, Mäder U (2013). Duration, frequency, and types of children's activities: Potential of a classification procedure. *Journal of Exercise Science & Fitness*, 11: 85–94.

Sadrizadeh S, Yao R, Yuan F, et al. (2022). Indoor air quality and health in schools: A critical review for developing the roadmap for the future school environment. *Journal of Building Engineering*, 57: 104908.

Sangsuwan K, Ekpanyapong M (2024). Video-based vehicle speed estimation using speed measurement metrics. *IEEE Access*, 12: 4845–4858.

Shaddick G, Thomas ML, Mudu P, et al. (2020). Half the world's population are exposed to increasing air pollution. *NPJ Climate and Atmospheric Science*, 3: 23.

Shirazi MS, Morris B (2015). Observing behaviors at intersections: A review of recent studies & developments. In: Proceedings of the 2015 IEEE Intelligent Vehicles Symposium (IV), Seoul, Korea, pp. 1258–1263.

Sigmund E, De Ste Croix M, Miklánková L, et al. (2007). Physical activity patterns of kindergarten children in comparison to teenagers and young adults. *European Journal of Public Health*, 17: 646–651.

Slezakova K, Peixoto C, Oliveira M, et al. (2018). Indoor particulate pollution in fitness centres with emphasis on ultrafine particles. *Environmental Pollution*, 233: 180–193.

Slezakova K, de Oliveira Fernandes E, do Carmo Pereira M (2019). Assessment of ultrafine particles in primary schools: Emphasis on different indoor microenvironments. *Environmental Pollution*, 246: 885–895.

Slezakova K, Pereira MC, Morais S (2020). Ultrafine particles: Levels in ambient air during outdoor sport activities. *Environmental Pollution*, 258: 113648.

Son YS (2023). A review on indoor and outdoor factors affecting the level of particulate matter in classrooms of elementary schools. *Journal of Building Engineering*, 75: 106957.

Song H, Zhang X, Song J, et al. (2023). Detection and tracking of safety helmet based on DeepSort and YOLOv5. *Multimedia Tools and Applications*, 82: 10781–10794.

Tao Y, Inthavong K, Tu J (2017a). Computational fluid dynamics study of human-induced wake and particle dispersion in indoor environment. *Indoor and Built Environment*, 26: 185–198.

Tao Y, Inthavong K, Tu JY (2017b). Dynamic meshing modelling for particle resuspension caused by swinging manikin motion. *Building and Environment*, 123: 529–542.

Telford A, Salmon J, Timperio A, et al. (2005). Quantifying and characterizing physical activity among 5- to 6- and 10- to 12-year-old children: The children's leisure activities study (CLASS). *Pediatric Exercise Science*, 17: 266–280.

Tikul N, Hokpunna A, Chawana P (2022). Improving indoor air quality in primary school buildings through optimized apertures and classroom furniture layouts. *Journal of Building Engineering*, 62: 105324.

Turaga P, Chellappa R, Subrahmanian VS, et al. (2008). Machine recognition of human activities: A survey. *IEEE Transactions on Circuits and Systems for Video Technology*, 18: 1473–1488.

Ul-Saufie AZ, Yahya AS, Ramli NA, et al. (2011). Comparison between multiple linear regression and feed forward back propagation neural network models for predicting PM10 concentration level based on gaseous and meteorological parameters. *International Journal of Applied Science and Technology*, 1: 42–49.

Um CY, Zhang N, Kang K, et al. (2022). Occupant behavior and indoor particulate concentrations in daycare centers. *Science of The Total Environment*, 824: 153206.

US Department of Health and Human Services (2018). Physical Activity Guidelines for Americans, 2nd edition.

Villanueva F, Notario A, Cabañas B, et al. (2021). Assessment of CO_2 and aerosol ($PM_{2.5}$, PM_{10}, UFP) concentrations during the reopening of schools in the COVID-19 pandemic: The case of a metropolitan area in Central-Southern Spain. *Environmental Research*, 197: 111092.

Wang L (2019). Accelerometer-determined physical activity of children during segmented school days: The Shanghai perspective. *European Physical Education Review*, 25: 816–829.

Wang CY, Liao HM, Yeh IH (2022). Designing network design strategies through gradient path analysis. arXiv Preprint. Available at https://arxiv.org/abs/2211.04800.

Wang CY, Bochkovskiy A, Liao HM (2023). YOLOv7: Trainable bag-of-freebies sets new state-of-the-art for real-time object detectors. In: Proceedings of the 2023 IEEE/CVF Conference on Computer Vision and Pattern Recognition, Vancouver, BC, Canada, pp. 7464–7475.

Wang W, Wang X, Li X, et al. (2024a). Seasonal particle size distribution and its influencing factors in a typical polluted city in North China. *Aerosol and Air Quality Research*, 24: 230127.

Wang CY, Yeh IH, Liao HM (2024b). YOLOv9: Learning what you want to learn using programmable gradient information. arXiv Preprint. Available at https://arxiv.org/abs/2402.13616.

Wojke N, Bewley A, Paulus D (2017). Simple online and realtime tracking with a deep association metric. In: Proceedings of the 2017 IEEE International Conference on Image Processing, Beijing, China, pp. 3645–3649.

Xie Z, Wang L, Chen H, et al. (2024). Accelerometer-measured sedentary volume and bouts during the segmented school day among Chinese school students. *Journal of Exercise Science & Fitness*, 22: 145–151.

Xu H, Guinot B, Cao J, et al. (2018). Source, health risk and composition impact of outdoor very fine particles (VFPs) to school indoor environment in Xi'an, Northwestern China. *Science of The Total Environment*, 612: 238–246.

Yang G, Zhou Y, Yan B (2023). Contribution of influential factors on $PM_{2.5}$ concentrations in classrooms of a primary school in North China: A machine discovery approach. *Energy and Buildings*, 283: 112787.

Yu JJQ, Gu J (2019). Real-time traffic speed estimation with graph convolutional generative autoencoder. *IEEE Transactions on Intelligent Transportation Systems*, 20: 3940–3951.

Yuan F, Yao R, Yu W, et al. (2023). Dynamic characteristics of particulate matter resuspension due to human activities in indoor environments: A comprehensive review. *Journal of Building Engineering*, 79: 107914.

Yuan F, Yao R, Sadrizadeh S, et al. (2024). The influence of activity patterns and relative humidity on particle resuspension in classrooms. *Science of The Total Environment*, 946: 173898.

Zhang Z (2000). A flexible new technique for camera calibration. *IEEE Transactions on Pattern Analysis and Machine Intelligence*, 22: 1330–1334.

Zhang Y, Shengxia M, Chang C, et al. (2017). Physical activity guidelines for Chinese children and youth. *Chinese Journal of Evidence-Based Pediatrics*, 12: 401–409. (in Chinese)

Zhong X, Ridley IA (2020). Verification of behavioural models of window opening: The accuracy of window-use pattern, indoor temperature and indoor $PM_{2.5}$ concentration prediction. *Building Simulation*, 13: 527–542.

Zhou Y, Yang G, Li X (2021). Indoor $PM_{2.5}$ concentrations and students' behavior in primary school classrooms. *Journal of Cleaner Production*, 318: 128460.

Zhu H, Wei H, Li B, et al. (2020). A review of video object detection: Datasets, metrics and methods. *Applied Sciences*, 10: 7834.

Zhu Y, Li X, Fan L, et al. (2021). Indoor air quality in the primary school of China—Results from CIEHS 2018 study. *Environmental Pollution*, 291: 118094.